A versatile QCM matrix system for online and high-throughput bio-sensing

G. Steve Huang,* Menq-Te Wang and Meng-Yen Hong

Received 7th November 2005, Accepted 20th December 2005
First published as an Advance Article on the web 13th January 2006
DOI: 10.1039/b515722f

A 3 × 3 quartz crystal microbalance (QCM) sensor matrix, fabricated on an A-T cut quartz crystal, has the ability to detect online a variety of labeled DNA samples in a parallel and comparative fashion. The QCM matrix was equipped with a single oscillator circuit, which activated only one QCM at any given time, and was controlled by programmable time-shared electronic relays. The gold electrode had a diameter of 0.8 mm and operated at a fundamental resonating frequency of 40 MHz; the dimensions of the matrix were 1.2 cm × 1.2 cm. The sensitivity of an individual QCM was in the pictogram regime. Selected QCMs were coated with either streptavidin or the anti-DIG antibody; the specificity of their detections was monitored using various concentrations of samples of biotin- and DIG-labeled DNA. The basic design of the QCM matrix is readily expandable, without any conceivable difficulties, in both geometry and circuitry.

Introduction

A quartz crystal microbalance (QCM) is a mass-detection device that operates based on the piezoelectric properties of quartz crystals. Because of their extraordinary sensitivity and stability, QCMs have been applied in recent years as biosensors for the online detection of biomolecules.[1,2] Molecular imprinting technologies have been combined with QCMs to allow the detection of terpenes,[3] caffeine,[4] and lysozyme.[5] Layer-by-layer studies for proteins and DNA also have been investigated using QCMs.[6–14] QCMs have also played pivotal roles in the recent development of biomimetric systems,[15–21] studies of biochemical processes[22–31] and protein–protein interactions,[32–37] the detection of single herpes virus,[38–41] detection of single-base DNA mutations,[42] and drug discovery.[1]

In addition to the broad-spectrum applications of single-well devices, effort has been exerted to develop high-throughput designs having flow injection analysis (FIA) capability. Five sets of QCM/oscillator (QMC-OSC) systems have been organized with one frequency counter for the detection of gases;[43] this system is capable of performing parallel detection in the expanse of space. In a similar design, a multichannel counter that monitors eight QCM-OSCs has been assembled to discriminate between the substances present in the breath of individuals suffering from halitosis.[44] One particularly brilliant design contains six QCMs and a computer-controlled relay system that performs simultaneous detection in a composter.[45] Even with these advances, however, the space-consuming QCM arrays are still a long way from being used in high-throughput applications.

If QCMs are to be used in high-throughput applications, both their hardware and software must be re-designed. The most-simple design is to arrange the QCMs in a matrix conformation in which the upper electrodes of the QCM are interconnected vertical lines (x-index) and the lower electrodes are linked by horizontal lines (y-index); thus, each QCM is addressed by a specific combination of x and y. The practical addressing is achieved through PC-controlled commands that provide information regarding the values of x and y and the duration in seconds. The advantage of this design is the use of a simplified resonating circuit; thereafter, only a single frequency counter is required. To validate this concept, we developed a 3 × 3 QCM matrix system equipped with a time-resolved relay. We encased this fabricated QCM matrix in a flow-cell system for the detection of DNA in solution. Such a QCM system has the potential of expanding to incorporate an almost unlimited number of QCM sensor matrixes for the online detection of specific biomolecules.

Institute of Nanotechnology, National Chiao Tung University, Hsinchu 300, Taiwan. E-mail: gstevehuang@mail.nctu.edu.tw; Fax: +886-3-5753956; Tel: +886-3-5131451

Experimental

Materials

The oscillator (Catalog # 35366-10) and flow cell (Catalog # 35363) were purchased from International Crystal Manufacturing Co. (Oklahoma City, USA). The QCM was fabricated from a 0.2 mm-thick AT-cut quartz wafer. A laboratory-constructed transistor–transistor logic integrated circuit (TTL-IC) was used to power the QCM. The TTL-IC was based on IC 74HC93, 74LS138, 74LS95, 74LS04 and D1A050000 and D1C050000 relays (KUAN HIS Co.). An Agilent HP 53132 Universal Frequency Counter was used to monitor the frequency output.

Biotin-16-2′-deoxy-uridine-5′-triphosphate (Biotin-16-dUTP), digoxigenin-11-2′-deoxy-uridine-5′-triphosphate (DIG-11-dUTP), streptavidin conjugate of β-galactosidase (St-β-gal), and anti-digoxigenin antibody conjugated to alkaline phosphatase (anti-DIG-AP) were purchased from Roche Diagnostics GmbH, Germany. Other chemicals were of analytical grade and were purchased from Sigma or Merck.

Cleaning and coating of gold electrode

The gold electrode was cleaned by immersion in 1.2 M NaOH for 20 min, 1.2 M HCl for 5 min, and distilled water for 5 min;

after a final rinse with 95% alcohol it was air-dried at room temperature.[9] For activation, the gold electrodes were treated with 2.5% glutaraldehyde (0.5 μL) for 15 min, washed briefly with distilled water, and then dried. A sample of St-β-gal or anti-DIG-AP (2 μL) was applied to the pretreated gold electrode and incubated in a humid hood for 100 min. For the preparation of control QCMs, bovine serum albumin (BSA; 1 mg mL^{-1}, 0.5 μL) was applied instead. The coated electrodes were washed thoroughly with double-distilled water, followed by a PBS wash. Blocking was achieved by adding BSA (1 mg mL^{-1}, 0.5 μL), incubating in a humid hood for 1 h, washing with water, rinsing with PBS, and then air-drying. The coating efficiency for St-β-gal was obtained through a coloring assay: dropping 1 μL X-gal substrate (1.2 mM 5-bromo-4-chloro-3-indolyl β-D-galactopyranoside, 1 mM $MgCl_2$, 3 mM $K_3Fe(CN)_6$, 3 mM $K_4Fe(CN)_6$ in PBS) onto the coated surface and measure the absorbance at 430 nm. The coating efficiency for anti-DIG-AP was also obtained through a coloring assay: dropping 1 μL of Fast red TR/naphthol AS-MX substrate (Pierce, Rockfod, IL) onto the coated surface and measure the absorbance at 550 nm. The coated QCM was assembled in a flow cell through which PBS was passed at a flow rate of 1 mL h^{-1}. The frequencies of all of the QCMs were monitored until steady state conditions were achieved (usually 30 min to 1 h).

PCR-labeled DNA

A Bluescipt-based plasmid containing a human L18 cDNA fragment (1 kb in length) inserted at multiple cloning sites was used as a template for PCR amplification. The sequences of the primers were 5′CTG CAA GGC GAT TAA GTT GGG TAA3′ and 5′GTG AGC GGA TAA CAA TTT CAC ACA CGA AAC AGC3′. The PCR amplifications were performed using purified plasmid (10 ng) in a sample (total volume: 100 μL) containing 10 mM Tris-HCl (pH 8.8), 1.5 mM $MgCl_2$, 50 mM KCl, 0.1% Triton X-100, 200 μM dNTP, 0.2 μM of each primer, and 0.5 units of Taq polymerase (Viogen Co., Taiwan). For labeled DNA, 5 μM DIG-11-dUTP or 5 μM biotin-16-dUTP was also incorporated. The thermal cycle program was as follows: preheat at 95 °C for 10 min; 25 repeated thermal cycles of 95 °C for 30 s, 57 °C for 30 s, and then 72 °C for 4 min; extension, 10 min at 72 °C. The lengths of the PCR products were verified through 1% agarose gel electrophoresis using suitably size markers. Unreacted small molecules were removed through Millipore MultiScreen-HV plate filtration (Millipore Co., USA). The concentration of DNA was quantified through UV absorbance measurements at 260 nm; the final concentration was adjusted to 1 ng μL^{-1}.

Results and discussion

QCM matrix FIA system

A 3 × 3 QCM matrix was fabricated on a 0.2 mm-thick AT-cut quartz wafer (Fig. 1). The diameter of each electrode was 0.8 mm. All electrodes were placed in a 1 cm × 1 cm area that fitted into the flow-cell unit. The top electrodes were 100 nm-thick gold layers; the bottom electrodes were aluminium layers of the same thickness. In this conformation, each QCM in the matrix was addressable through a single combination of X- and Y-lines.

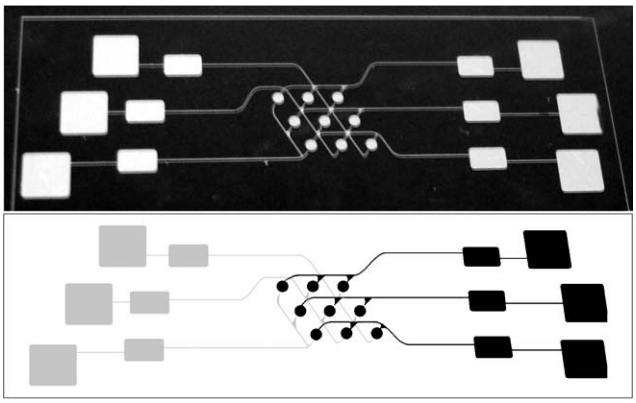

Fig. 1 A 3 × 3 QCM matrix fabricated on a quartz wafer. The upper image is a photograph of the fabricated matrix. The top electrodes are gold-plated; the bottom electrodes are aluminium. Blurring in this image was caused by reflection of the wafer. The lower image is a schematic drawing depicting details of the matrix's construction.

To selectively activate a single QCM at any given time, a programmable, PC-controlled switching circuit was constructed using six DIA050000 electronic relays (Fig. 2). During the on/off cycle of each QCM, residual charges remaining on the QCM created extra noise and caused signal decay. To reduce the residual charge, two DIC050000 devices were incorporated in the relay system. Discharging of all the QCMs was activated during the intervals between each QCM resonance. In practice, each QCM was turned on for 0.9 s followed by discharging for 0.1 s (Table 1). The complete cycle took 9 s.

We adopted a standard oscillating circuit design (Fig. 3) and used an Agilent HP 53132 Universal Frequency Counter to monitor the frequency output. Because of the presence of the electronic relay system, only one set of oscillators/counters was required. We constructed a QCM matrix FIA system consisting of a QCM matrix in the flow-cell, a cylindrical pump, an injector, a PC-controlled electronic relay circuit, an oscillator circuit, and a frequency counter (Fig. 3).

To record and display the frequency response of each QCM simultaneously, we used LabView (National Instrument Co.) to control the switching of electronic relays through a DIO D/D control card, receive resonant frequency from an Agilent 53132A through GPIB CARD (National Instruments Corporation.), and graphically display the frequency recordings from the nine QCMs in a single window on the computer's screen (Fig. 4).

The QCM oscillating circuit was operated at a fundamental resonating frequency of 40 MHz. The frequency shift corresponding to the applied weight for individual QCM in the matrix displayed sensitivity in the picogram regime (Fig. 5). The dynamic (linear) range in terms of frequency shift *vs.* applied weight/mass loading is given as an inset (Fig. 5 inset). According to the Sauerbrey equation:

$$\Delta f = -2f_0 \times 2\Delta m/A(\mu_q\rho_q)^{1/2}$$

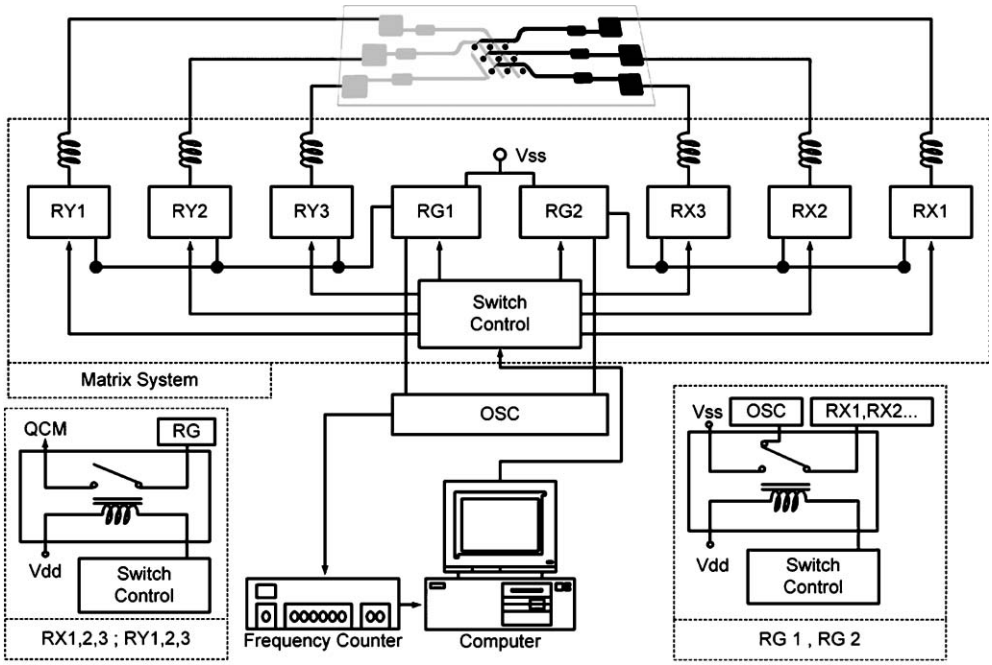

Fig. 2 Schematic representation for the switching mechanism that selectively activates each QCM in the matrix. The heart of the switching process is the operation of six DIA050000 electronic relays (RX1, RX2, RX3, RY1, RY2, and RY3) that control the values of X1, X2, X3, Y1, Y2, and Y3 for the QCM matrix. A circuit diagram is depicted in the upper left-hand corner. Two electronic relays DIC050000 (RG1 and RG2) discharge residual charges on the QCM between on/off cycles and are depicted in the bottom right-hand corner. The switching motion is controlled, and the frequency recorded, by a personal computer.

where Δf, Δm are the frequency and mass change, A is the piezoelectric active area, μ_q is the shear modulus, ρ_q is the density of quartz. Frequency shifts induced by 10^{-7} g should be 3 order higher than frequency shifts induced by 10^{-10} g; however in our experiment, the difference was only ten. This might be due to defects caused by the etching process, or a non-uniform pattern width caused by the lift-off process.

Detection of labeled DNA

Specific detection of DNA molecules was achieved through antigen–antibody binding or biotin–streptavidin binding. DIG is incorporated into DNA molecules and detected by the coated anti-DIG antibody. Biotin is incorporated into DNA molecules and detected by the coated streptavidin. To perform the detection of a specific DNA sample, we coated selected QCMs with St-β-gal (QCM1, QCM5) and anti-DIG-AP (QCM2, QCM6). The remaining QCMs were coated with BSA; they served as controls. Injection of 1 ng of BSA did not induce a frequency shift for any of the QCMs in the matrix (Fig. 6B). Injection of 1 ng of biotin-labeled L18 DNA induced frequency shifts of 21 Hz for QCM1 and 16 Hz for QCM5 (Fig. 6C). The difference between the frequency shifts of QCM1 and QCM5 probably was due to the dead volume of the flow cell (*ca.* 100 μL), resulting from the time lapse (*ca.* 60 s) between the two detections. Initially, the injected DNA bound to QCM1 and then diluted into the flow cell before binding to QCM5. The local concentration at QCM1 was much higher than that at QCM5 and, thus, it quickly saturated the binding sites on QCM1. Neither the BSA-coated QCMs

Table 1 Typical program of relays that control the on/off states of individual QCMs in the matrix

Step	1	2	3	4	5	6	7	8	9	10	11	12	13	14	15	16	17	18
RX1[a]	1	1	0	1	0	1	1	1	0	1	0	1	1	1	0	1	0	1
RX2	0	1	1	1	0	1	0	1	1	1	0	1	0	1	1	1	0	1
RX3	0	1	0	1	1	1	0	1	0	1	1	1	0	1	0	1	1	1
RY1	1	1	1	1	1	1	0	1	0	1	0	1	0	1	0	1	0	1
RY2	0	1	0	1	0	1	1	1	1	1	1	1	0	1	0	1	0	1
RY3	0	1	0	1	0	1	0	1	0	1	0	1	1	1	1	1	1	1
RG1	0	1	0	1	0	1	0	1	0	1	0	1	0	1	0	1	0	1
RG2	0	1	0	1	0	1	0	1	0	1	0	1	0	1	0	1	0	1
QCM in action	Q1	—	Q2	—	Q3	—	Q4	—	Q5	—	Q6	—	Q7	—	Q8	—	Q9	—

[a] The activation of QCM in the matrix is controlled through the electronic relay to be "on" (1) or "off" (0). Each column depicts the on/off status of the relays. RX1, RX2, and RX3 control the wires connecting X1, X2, and X3, respectively. RY1, RY2, and RY3 control the wires connecting Y1, Y2, and Y3, respectively. RG1 and RG2 control the discharging circuit. A complete cycle is composed of a total of 18 steps. Odd-numbered steps (1, 3, 5, 7, 9, 11, 13, 15, and 17) correspond to the activation of the indicated QCM; they lasted 0.9 s. Even-numbered steps switched on the discharging action; they lasted 0.1 s. A complete cycle took 9 s.

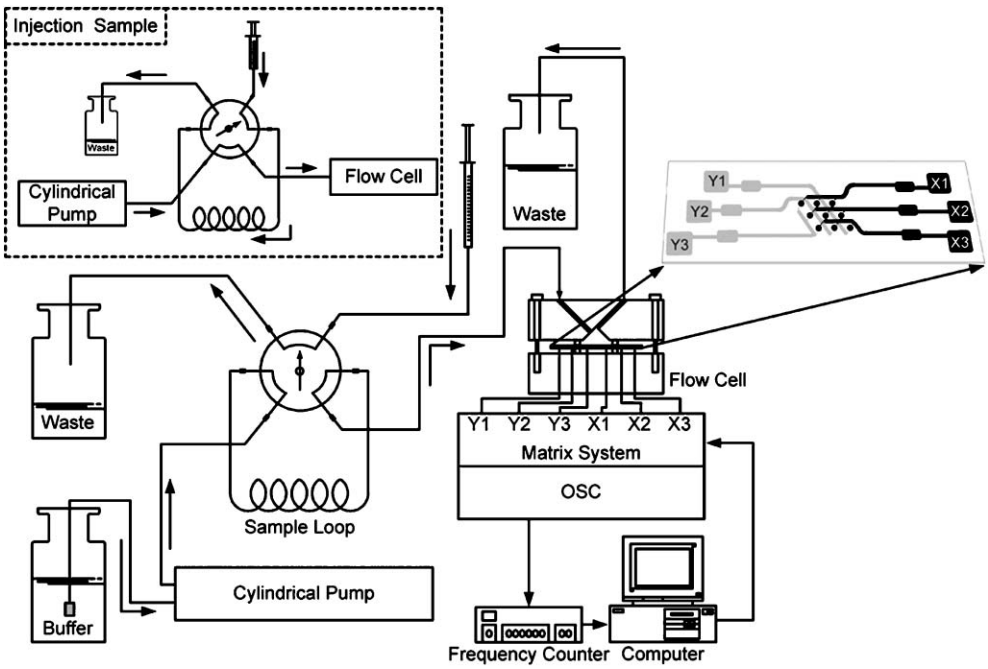

Fig. 3 Schematic illustration of the 3 × 3 matrix QCM flow injection analysis apparatus. Continuous flow was achieved using a cylindrical pump. The sample was injected through an injection loop and pumped into the flow cell containing the coated 3 × 3 QCM matrix. The oscillator (OSC) activates the designated QCM selectively through a matrix control system and the resonant frequency is measured and reported back to the PC.

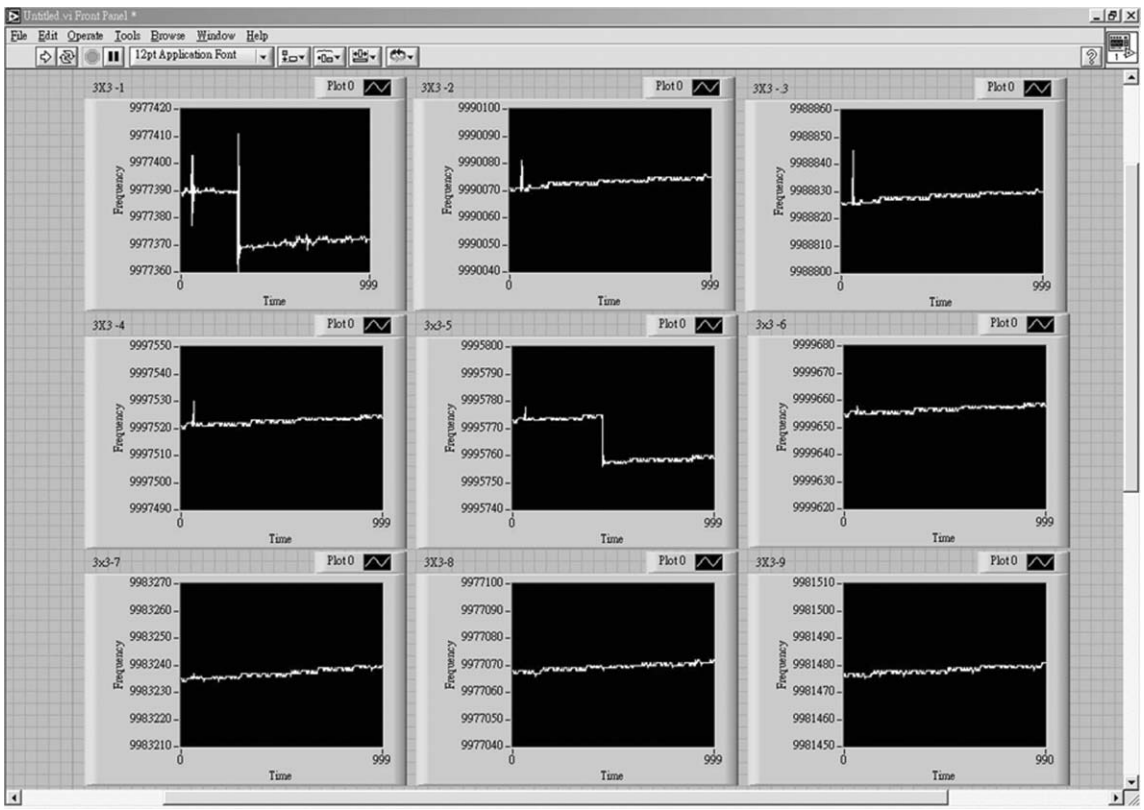

Fig. 4 Screen-capture image of the LabView-controlled QCM matrix for the online monitoring of DNA detection.

nor the anti-DIG IgG-coated QCMs displayed a significant difference in frequency shift. The injection of 1 ng of DIG-labeled L18 DNA into the matrix was detected by QCM2 (14 Hz) and QCM6 (13 Hz) (Fig. 6D). These lower responses in terms of frequency, relative to those of the biotin-labeled DNA, are probably due to the lower number of binding sites

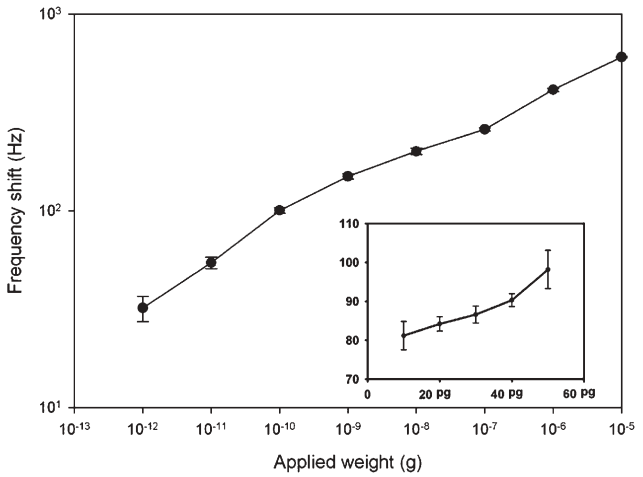

Fig. 5 Typical frequency response of the QCM selected from the matrix.

on the anti-DIG-coated QCM. Differences in local concentrations were also observed from this latter injection.

We also performed repeated stripping and coating to QCM matrixes and observed the quality response. No significant difference was observed between repeated stripping up to 10 times.

A number of factors must be considered when attempting to expand the number of QCMs in such a matrix design. When the number of QCMs increases, the time shared by each QCM decreases proportionally. The time required for relay switching, the time required for the oscillations to build up and stabilize, the time required to reach a stable frequency reading, and the time required for sufficient discharging are all important factors that determine the number of QCMs that can be incorporated. In practice, the current matrix is restricted by the manufacture's design of frequency counter that acquires and provides stable frequency reading in the subsecond range. The utilization of tens of thousands of QCMs in such a matrix would require the incorporation of a much-faster acquisition mechanism. Discharging is another limiting factor that is encountered only in a matrix configuration. Residual charges on the QCM confuse the oscillation circuit and cause signal reduction, decay, noise, and, sometimes, an inability to oscillate. When the number of QCMs increases, the electrode area decreases significantly; thus, the time required for discharging might be reduced dramatically. The actual length of time required for discharging in a different design, however, remains purely empirical.

Conclusions

We have demonstrated the application of a versatile QCM matrix system that behaves as a specific biosensor. The detection is simultaneous, parallel, and comparative. In this present study, we provide a possible route toward the future application of matrix sensors in proteomics, genomic research, and drug discovery applications.

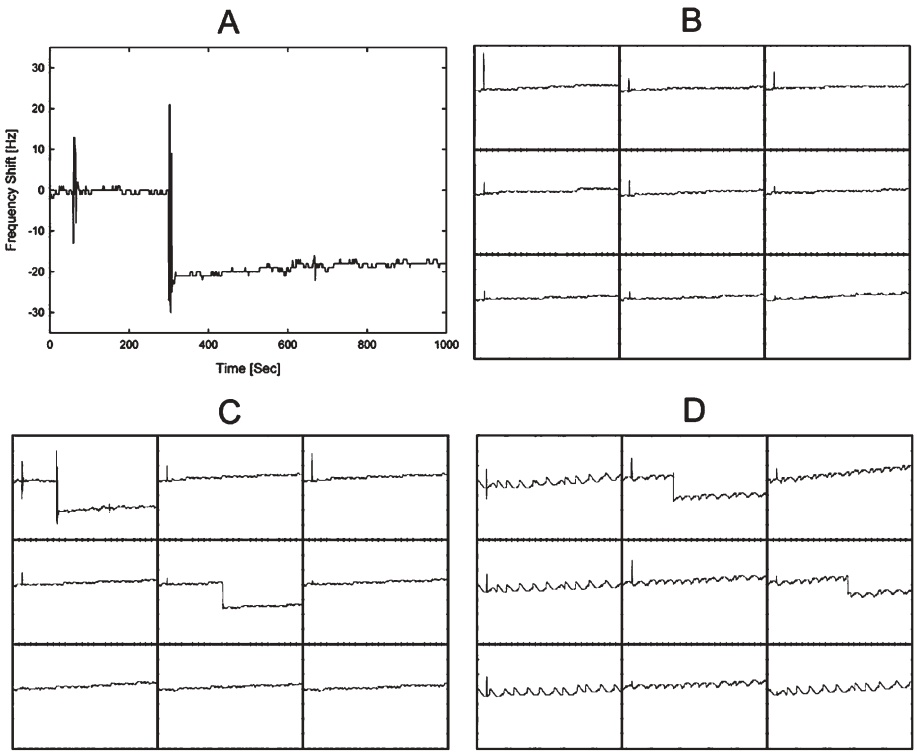

Fig. 6 Specific detection of labeled DNA samples using the QCM matrix. (A) Recording of the response of QCM1 to the injection of 1 ng of biotin-labeled L18 DNA. (B) Simultaneous recordings of nine QCM matrixes after 1 ng of BSA had been injected. (C) Simultaneous recordings after the injection of 1 ng of biotin-labeled L18 DNA. (D) Simultaneous recordings of the injection of 1 ng of DIG-labeled L18 DNA. Sequence of QCMs (from left to right): (top) QCM1, QCM2, and QCM3; (center) QCM4, QCM5, and QCM6; (bottom) QCM7, QCM8, and QCM9.

Acknowledgements

We thank Ms Li-Wen Huang for her artistic contribution in the preparation of the illustrated contents entry. This study was supported in part by National Science Council Grants NSC 93-2314-B-039-018 and NSC94-2320-B-009-003.

References

1 B. A. Cavic, G. L. Hayward and M. Thompson, *Analyst*, 1999, **124**, 1405–1420.
2 K. A. Marx, *Biomacromolecules*, 2003, **4**, 1099–1120.
3 C. J. Percival, S. Stanley, M. Galle, A. Braithwaite, M. I. Newton, G. McHale and W. Hayes, *Anal. Chem.*, 2001, **73**, 4225–4228.
4 T. Kobayashi, Y. Murawaki, P. S. Reddy, M. Abe and N. Fujii, *Anal. Chim. Acta*, 2001, **435**, 141–49.
5 K. Hirayama, Y. sakai and K. kameoka, *J. Appl. Polym. Sci.*, 2001, **81**, 3378–3387.
6 P. He, N. Hu and G. Zhou, *Biomacromolecules*, 2002, **3**, 139–146.
7 T. Nonogaki, S. Xu, S.-i. Kugimiya, S. Sato, I. Miyata and M. Yonese, *Langmuir*, 2000, **16**, 4272–4278.
8 I. Galeska, T. Hickey, F. Moussy, D. Kreutzer and F. Papadimitrakopoulos, *Biomacromolecules*, 2001, **2**, 1249–1255.
9 E. S. Forzani, V. M. Solis and E. J. Calvo, *Anal. Chem.*, 2000, **72**, 5300–5307.
10 E. J. Calvo, F. Battaglini, C. Danilowicz, A. Wolosiuk and M. Otero, *Faraday Discuss.*, 2000, **116**, 47–65.
11 E. J. Calvo, R. Etchenique, L. Pietrasanta, A. Wolosiuk and C. Danilowicz, *Anal. Chem.*, 2001, **73**, 1161–1168.
12 E. R. Welsh, C. L. Schauer, J. P. Santos and R. R. Price, *Langmuir*, 2004, **20**, 1807–1811.
13 R. MK, B. P, D. H, P. S and N. C, *Biosens. Bioelectron.*, 2001, **16**, 849–856.
14 A. Baba, F. K. c and R. C. Advincula, *Colloids Surf., A*, 2000, **173**, 39–49.
15 S. Nakata, n. kido, M. Hayashi, M. Hara, H. Sasabe, T. Sugawara and T. Matsuda, *Biophys. Chem.*, 1996, **62**, 63–72.
16 F. Hook, M. Rodahl, P. Brzezinski and B. Kasemo, *Langmuir*, 1998, **14**, 729–734.
17 F. Hook, B. Kasemo, T. Nylander, C. Fant, K. Sott and H. Elwing, *Anal. Chem.*, 2001, **73**, 5796–5804.
18 A. Kobayashi, Y. Sato and F. Mizutani, *Biosci., Biotechnol., Biochem.*, 2001, **65**, 2392–2396.
19 S. Fukuoka and I. Karube, *Appl. Biochem. Biotechnol.*, 1994, **49**, 1–9.
20 H.-C. Chang, C.-C. Yang and T.-M. Yeh, *Anal. Chim. Acta*, 1997, **340**, 49–54.
21 M. Liebau, A. Hildebrand and R. H. Neubert, *Eur. Biophys. J.*, 2001, **30**, 42–52.
22 K. Ito, K. Hashimoto and Y. Ishimori, *Anal. Chim. Acta*, 1996, **327**, 29–35.
23 R. B. Towery, N. C. Fawcett, P. Zhang and J. A. Evans, *Biosens. Bioelectron.*, 2001, **16**, 1–8.
24 I. Okahata, K. Niikura, H. Furusawa and H. Matsuno, *Anal. Sci.*, 2000, **16**, 1113–1119.
25 H. Su, M. Yang, K. M. R. Kallury and M. Thompson, *Analyst*, 1993, **118**, 309–312.
26 L. M. Furtado and M. Thompson, *Analyst*, 1998, **123**, 1937–1945.
27 H. Su, S. Chong and M. Thompson, *Langmuir*, 1996, **12**, 2247–2255.
28 H. Su, P. Williams and M. Thompson, *Anal. Chem.*, 1996, **67**, 1010–1013.
29 Y. Wang, N. Farrell and J. D. Burgess, *J. Am. Chem. Soc.*, 2001, **123**, 5576–5577.
30 L. M. Furtado, H. Su, M. Thompson, D. P. Mack and G. L. Hayward, *Anal. Chem.*, 1999, **71**, 1167–1175.
31 H. Matsuno, K. Niikura and Y. Okahata, *Chemistry*, 2001, **7**, 3305–3312.
32 M. Thompson, C. L. Arthur and G. K. Dhaliwal, *Anal. Chem.*, 1986, **58**, 1206–1209.
33 M. Muratsugu, S. Kurosawat and N. Kamo, *Anal. Chem.*, 1992, **64**, 2403–2407.
34 S. Sakti, R. Lucklum, P. Hauptmann, F. Buhling and S. Ansorge, *Biosens. Bioelectron.*, 2001, **16**, 1101–1108.
35 Y. S. Fung and Y. Y. Wong, *Anal. Chem.*, 2001, **73**, 5302–5309.
36 A. J.-C. Eun, L. Huang, F. T. Chew, S. F.-Y. Li and S. M. Wong, *J. Virol. Methods*, 2002, **99**, 71–79.
37 X. Zhou, L. Liu, M. Hu, L. Wang and J. Hu, *J. Pharm. Biomed. Anal.*, 2002, **27**, 341–345.
38 E. Uttenthaler, M. Schraml, M. Johannes and D. Stephan, *Biosens. Bioelectron.*, 2001, **16**, 735–743.
39 F. N. Dultsev, R. E. Speight, M. T. Fiorini, J. M. Blackburn, C. Abell, V. P. Ostanin and D. Klenerman, *Anal. Chem.*, 2001, **73**, 3935–3939.
40 A. J. Eun, L. Huang, F. T. Chew, S. F. Li and S. M. Wong, *J. Virol. Methods*, 2002, **99**, 71–79.
41 M. A. Cooper, F. N. Dultsev, T. Minson, V. P. Ostanin, C. Abell and D. Klenerman, *Nat. Biotechnol.*, 2001, **19**, 833–837.
42 F. Patolsky, A. Lichtenstein and I. Willner, *Nat. Biotechnol.*, 2001, **19**, 253–257.
43 R. Ni, X.-B. Zhang, W. Liu, G.-L. Shen and R.-Q. Yu, *Sens. Actuators, B*, 2003, **88**, 198–204.
44 J. Ito, T. Nakamotob and H. Uematsu, *Sens. Actuators, B*, 2004, **99**, 431–436.
45 F. L. Dickert, P. A. Lieberzeit, P. Achatz, C. Palfinger, M. Fassnauer, E. Schmid, W. Werther and G. Horner, *Analyst*, 2004, **129**, 432–437.